Transcriptome profiling of kenaf (*Hibiscus cannabinus L.*) under plumbic stress conditions implies the involvement of NAC transcription factors regulating reactive oxygen species-dependent programmed cell death

Xia An[1], Jie Chen[2] and Guanrong Jin[1]

[1] Zhejiang Academy of Agricultural Sciences, Hangzhou, China
[2] Huazhong Agricultural University, Wuhan, China

ABSTRACT

Heavy metal contamination of soils has become a serious global issue, and bioremediation has been proposed as a potential solution. Kenaf (*Hibiscus cannabinus* L.) is a fast growing, non-woody multipurpose annual plant that is suitable for removing excess heavy metals from soils. However, there has been relatively little research on the kenaf molecular mechanisms induced in response to an exposure to heavy metal stress. Thus, whole kenaf seedlings grown under control (normal) and stress (plumbic treatment) conditions were sampled for transcriptome sequencing. Unigenes generated through the *de novo* assembly of clean reads were functionally annotated based on seven databases. Transcription factor (TF)-coding genes were predicted and the physiological traits of the seedlings were analyzed. A total of 44.57 Gb high-quality sequencing data were obtained, which were assembled into 136,854 unigenes. These unigenes included 1,697 that were regarded as differentially expressed genes (DEGs). A GO enrichment analysis of the DEGs indicated that many of them are related to catalytic activities. Moreover, the DEGs appeared to suggest that numerous KEGG pathways are suppressed (e.g., the photosynthesis-involving pathways) or enhanced (like the flavonoid metabolism pathways) in response to Pb stress. Of the 2,066 predicted TF-coding genes, only 55 were differentially expressed between the control and stressed samples. Further analyses suggested that the plumbic stress treatment induced reactive oxygen species-dependent programmed cell death in the kenaf plants via a process that may be regulated by the differentially expressed NAC TF genes.

Subjects Cell Biology, Molecular Biology, Plant Science
Keywords Kenaf, Fiber crop, Plumbic stress, NAC, Transcription factors

Submitted 21 October 2019
Accepted 11 February 2020
Published 10 March 2020

Corresponding author
Xia An, anxia111@126.com

Academic editor
Kun Lu

Additional Information and Declarations can be found on page 12

DOI **10.7717/peerj.8733**

INTRODUCTION

Heavy metal contamination has emerged as a common problem worldwide. In China, approximately 20% of the available cultivated land has been contaminated by heavy metals from industrial urban emissions and agricultural practices (*Deng et al., 2017*), which has

How to cite this article An X, Chen J, Jin G. 2020. Transcriptome profiling of kenaf (*Hibiscus cannabinus L.*) under plumbic stress conditions implies the involvement of NAC transcription factors regulating reactive oxygen species-dependent programmed cell death. *PeerJ* **8**:e8733 http://doi.org/10.7717/peerj.8733

decreased the usable land area and restricted the distribution of vegetation. Additionally, the bioaccumulation of heavy metals in plants and animals seriously harms the food chain and human health. Bioremediation, which may be useful for minimizing heavy metal contamination, involves the growth of high biomass plants that can accumulate high concentrations of heavy metals on contaminated land. Thus, selecting and breeding cultivars suitable for bioremediation and characterizing the mechanisms underlying the responses of such plants to contaminated conditions are necessary (*Xu et al., 2019*).

Kenaf (*Hibiscus cannabinus* L.) is a fast-growing, non-woody multipurpose annual plant species in the family Malvaceae. Kenaf fiber has multiple applications in diverse fields, and is included in textile and packing materials, pulp and paper, composite media, animal feed, as well as in potting, building, and filtration materials, while also being useful for board making and as a source of biomass energy (*Ayadi et al., 2011*). Several factors have made kenaf the third largest fiber crop, behind only cotton and jute. For example, it is an excellent source of cellulosic fiber, it can be used in numerous fiber-based products, it has ideal physical strength properties for pulp and paper, and the energy consumed and chemical input required for pulping and paper-making processes are lower for kenaf than for other comparable wood fibers (*Ayadi et al., 2011*). In addition to the importance of kenaf as a valuable fiber crop, it has been proposed as a suitable plant for bioremediation because of its rapid growth, large biomass, stress resistance, and adaptability (*Deng et al., 2017*). However, little is known regarding how kenaf plants respond to various heavy metal stresses.

Previous studies have investigated the physiological mechanisms mediating kenaf responses to cadmium (Cd) stress (*Deng et al., 2017*). Among the numerous analyzed physiological indices, the malondialdehyde (MDA) content was positively correlated with the Cd concentration and duration of the stress exposure. In another study, researchers proposed various physiological indices for monitoring the responses of two kenaf cultivars to Cd stress (*Li et al., 2013*). Similarly, the physiological responses of another two kenaf cultivars to chromium (Cr) stress were determined (*Ding et al., 2016*). These earlier investigations of the molecular mechanisms of kenaf plants induced by heavy metal stresses were conducted in a relatively low-throughput manner (*Li et al., 2013*; *Niu et al., 2018*). Additionally, omics approaches (e.g., transcriptomic or proteomic analyses) were mostly applied to investigate the molecular mechanisms of kenaf plants subjected to drought stress (*Niu et al., 2016*; *An et al., 2018*).

In this study, we examined kenaf responses to plumbic stress at the transcriptional level. A total of 44.57 Gb high-quality sequencing data were generated for the control and stressed kenaf seedlings and then de novo assembled into 193,978 transcripts from 136,854 unigenes. These unigenes encode 2,066 transcription factors (TFs) belonging to 53 TF families. Moreover, 55 TF genes from 20 TF families were differentially expressed. Further examination of kenaf seedlings revealed that reactive oxygen species (ROS)-dependent programmed cell death (PCD) was induced in response to plumbic stress, in a process that may be regulated by the differentially expressed NAC (NAM, no apical meristem; ATAF, Arabidopsis transcription activation factor; and CUC, cup-shaped cotyledon) TF genes. Therefore, identifying the differentially expressed NAC TF genes based on the

high-throughput data produced in this study may help clarify the molecular mechanisms involved in kenaf responses to plumbic stress.

MATERIALS AND METHODS

Plant materials

Kenaf cultivar H368 was obtained from Professor Defang Li (Institute of Bast Fiber Crops, Chinese Academy of Agricultural Sciences). Plants were grown under a 16-h light (28 °C)/8-h dark (25 °C) cycle, with a relative humidity close to 60% and a light intensity of 700 μmol m^{-2} s^{-1}. A pot culture experiment was completed, with each pot (eight cm height, seven cm diameter) filled with an equal weight of a soil mixture comprising red soil: humus: vermiculite (2:1:1, v/v/v). When the plants grew to a height of nine cm, they were treated with a lead concentration of 4,000 mg/kg ($Pb(NO_3)_2$ treatment solution). We re-applied 4,000 mg/kg of $Pb(NO_3)_2$ in each pot at one time according to the matrix. The application method was to dissolve $Pb(NO_3)_2$ in 1,000 ml ddH_2O and then pour into the potted soil. Control plants were treated with the same solution without $Pb(NO_3)_2$. Each treatment was completed with two replicates. Three kenaf seedlings per replicate were collected 24 h later. They were immediately frozen with liquid nitrogen and stored at −80 °C until analyzed.

RNA extraction, library preparation, and sequencing

Total RNA was extracted from the frozen kenaf samples with the TRIzol reagent (Invitrogen, CA, USA). The RNA quality was checked by gel electrophoresis and with the 2100 Bioanalyzer (Agilent, CA, USA) for subsequent analyses. For each biological replicate, cDNA libraries were constructed (i.e., CK1, CK2, Pb1, and Pb2) and sequenced. Briefly, poly-A mRNA was isolated from the total RNA with Magnetic Oligo (dT) Beads and fragmented. Double-stranded cDNA was synthesized with the SuperScript Double-Stranded cDNA Synthesis kit (Invitrogen) and a random hexamer primer (Illumina). After an end-repair and phosphorylation step with T4 DNA polymerase, Klenow DNA polymerase, and T4 polynucleotide kinase, the ends of the cDNA fragments were ligated to Illumina paired-end adapters with T4 DNA ligase. The libraries comprising 200 ± 25 bp cDNA fragments were sequenced with the HiSeq X Ten sequencing platform to produce PE150 reads.

Data assembly and annotation

Raw sequencing data were processed by removing low-quality reads and reads containing adapter or poly-N sequences. The remaining clean reads were used for all downstream analyses. Transcripts were *de novo* assembled with the default parameters of the Trinity software (*Grabherr et al., 2011*) and then further clustered into unigenes with the Corset software (*Davidson & Oshlack, 2014*). The unigenes were functionally annotated based on seven databases. Details regarding these databases, software, and parameters are listed in Table S1.

Quantification of gene expression levels and analysis of differential expression

The gene expression levels of each sample were estimated by mapping the clean reads to the assembled transcriptome with the default parameters of the RSEM (RNA-Seq by Expectation Maximization) software (*Li & Dewey, 2011*). The mapped read counts were then transformed to FPKM (fragments per kilobase of transcript sequence per million base pairs sequenced) values to evaluate the relative unigene expression levels (*Trapnell et al., 2010*). The differential expression induced by the control and Pb stress conditions was analyzed with the DESeq R package (version 1.10.1) (*Anders & Huber, 2010*), with adjusted $p < 0.05$. Enriched gene ontology (GO) terms among the differentially expressed genes (DEGs) were identified with the GOseq R package based on the Wallenius non-central hyper-geometric distribution (*Young et al., 2010*). Moreover, the enriched Kyoto Encyclopedia of Genes and Genomes (KEGG) pathways were identified with the KOBAS software (*Mao et al., 2005*). The predicted TF genes based on the Plant Transcription Factor Database (version 5.0) (http://planttfdb.cbi.pku.edu.cn/) were compared with the DEGs to detect the differentially expressed TF genes.

Quantitative real-time PCR (qRT-PCR)

Total RNA was extracted from whole kenaf seedlings subjected to normal (CK) or Plumbic (Pb) stress conditions with the RNAqueous Total RNA Isolation Kit (Ambion, USA). The RNA was used as the template to synthesize cDNA with the HiScript II Q RT SuperMix for qPCR (Vazyme, China). The cDNA was diluted 10-fold with sterile water and used for a qRT-PCR assay. The *GAPDH* gene identified in the current transcriptome sequencing analysis (Cluster-5711.64302) served as an internal reference control. The qRT-PCR assay was performed with the LightCycler 480II Real-Time PCR Detection System (Roche Ltd, USA). The 20- μL reaction mixture contained 10 μL ChamQ SYBR qPCR Master Mix (Vazyme), 2 μL cDNA template (from approximately 100 ng total RNA), and 0.5 μM forward and reverse primers (Table S2). The amplification parameters were as follows: 95 °C for 30 s; 40 cycles of 95 °C for 10 s and 60 °C for 30 s. Three independent experiments were completed to ensure the qRT-PCR data were reproducible. Relative gene expression levels were calculated according to the $2^{-\Delta\Delta CT}$ method (*Livak & Schmittgen, 2001*).

Examination of physiological traits

Physiological traits of the CK and stressed samples were examined by Comin Biotechnology Co. Ltd. (http://www.cominbio.com). Regarding MDA content measurements, the frozen samples were ground in liquid nitrogen and then homogenized in 10 volumes (v/w) of pre-cooled potassium phosphate buffer (containing Na_2HPO_4 and NaH_2PO_4; pH 7.0) on ice. Samples were centrifuged at 8,000× g for 10 min at 4 °C. A 0.1-mL aliquot of the supernatant was mixed with 0.3 mL 0.5% (w/v) thiobarbituric acid, which was dissolved in 5% (w/v) trichloroacetic acid, and the extract was boiled for 40 min and then immediately cooled in ice. After centrifuging at 12,000× g for 10 min, the absorbance of the supernatant was measured at 532 nm. The effect of non-specific turbidity was eliminated by subtracting the absorbance of the supernatant at 600 nm. The MDA content [nmol/g fresh weight

(FW)] was calculated with the following formula: 25. 8× (A_{532} − A_{600})/weight, in which A_{532} and A_{600} are the absorbances at 532 and 600 nm, respectively.

To measure the peroxidase (POD) and catalase (CAT) contents (i.e., antioxidant enzymes), 10 μL supernatant (generated from the pre-cooled potassium phosphate buffer) was mixed with 190 μL working solution, after which the absorbance was measured twice at 470 nm (for POD) or 240 nm (for CAT). The second measurement (A2) was taken 1 min after the first (A1). The working solution for measuring the POD content comprised guaiacol, sodium acetate, and hydrogen peroxide, whereas the working solution for determining the CAT content was the potassium phosphate buffer supplemented with hydrogen peroxide. The POD and CAT contents (U/g FW) were calculated with the following formulae: 40× (A2 − A1)/weight and 918× (A1 –A2)/weight, respectively.

To determine the proline (PRO) content, samples were homogenized in a pre-cooled salicyl-sulfonic acid solution, boiled for 10 min, and centrifuged at 10, 000× g for 10 min at 25 °C. The supernatant was collected and mixed with the working solution comprising ninhydrin, acetic acid, and phosphoric acid. The resulting solution was boiled for 30 min and then cooled. Methylbenzene was added and the solution was vortexed for 30 s. The absorbance of the upper layer of the solution was measured at 520 nm. The PRO content was calculated with the following formula: 38. 4× (A_{520} + 0.0021)/weight.

Statistical analyses

Data were analyzed with SPSS software (version 22.0) (SPSS, Chicago, IL, USA). Error bars represent the standard deviation. The significance of the differences in the data for the control and stressed samples was assessed with Student's *t*-test (with *, **, and *** corresponding to $p < 0.05$, $p < 0.01$, and $p < 0.001$, respectively).

RESULTS

Illumina sequencing and assembly

Young kenaf seedlings under CK or Pb stress conditions were separately collected in duplicate for the construction of four cDNA libraries. A correlation analysis on the transcriptomic output revealed the consistency in the data generated by the replicates of the control (CK1 and CK2) and stressed (Pb1 and Pb2) samples (Fig. S1). The overall sequencing results are presented in Table S3. A total of 297,123,462 clean reads (44.57 Gb) were obtained from our data. The error rates for all four samples were less than 0.1% and the Q30 values exceeded 94.66. These high-quality clean reads were assembled into transcripts with the Trinity software (*Grabherr et al., 2011*) and were further clustered into unigenes with the Corset software (*Davidson & Oshlack, 2014*). Consequently, 193,978 transcripts were generated, from which 136,854 unigenes were obtained. The unigenes comprised fewer total nucleotides, but were longer than the transcripts (Table S4 and Fig. 1).

Gene annotation and function classification

The assembled unigenes were functionally annotated based on the NCBI non-redundant protein sequence (Nr) database, the NCBI nucleotide sequence (Nt) database, the Protein

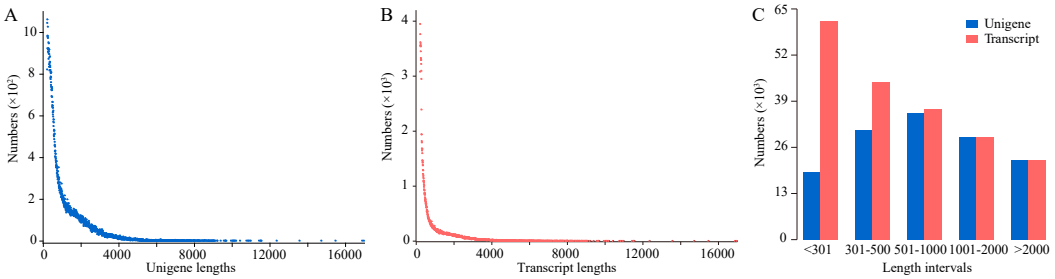

Figure 1 Analysis of transcript and unigene lengths. Length distribution of the assembled transcripts (A) and unigenes (B) are respectively presented, as well as the statistics regarding the number of sequences distributed on different lengths (C).

Full-size DOI: 10.7717/peerj.8733/fig-1

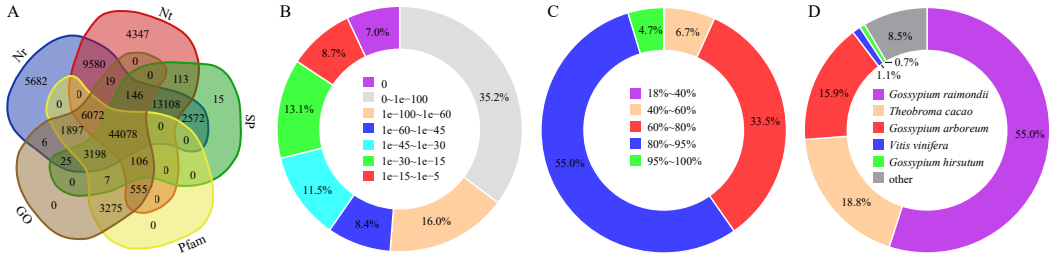

Figure 2 Statistics of unigene annotations. Venn diagram of the unigenes annotated based on five databases (A). Percentage distribution of E-values (B), sequence similarities (C), and top species annotated (D) following a BLAST search of the Nr database with the unigenes as queries. Nr, NCBI non-redundant protein sequence database; Nt, NCBI nucleotide sequence database; Pfam, Protein family database; KOG, euKaryotic Orthologous Groups database; SP, Swiss-Prot database.

Full-size DOI: 10.7717/peerj.8733/fig-2

family (Pfam) database, the euKaryotic Orthologous Groups (KOG) database, the Swiss-Prot (SP) database, the KEGG database, and the GO database. The number of unigenes annotated with each database is indicated in Table S5. Specifically, 32.21% of the unigenes were commonly annotated with the Nr, Nt, SP, Pfam, and GO databases (Fig. 2A). The *E*-value distribution for the unigenes annotated with the Nr database (i.e., the database with the most annotated unigenes; Table S5) indicated that 78.2% of the annotated unigenes (67,503 of 86,376) had E-values less than 1e−30 (Fig. 2B). Moreover, 93.2% of the unigenes annotated with the Nr database (80,485 of 86,376) matched genes in the database with ≥ 60% sequence similarities (Fig. 2C). Additionally, the unigenes were most similar to genes from ancestral cotton species (*Gossypium raimondii*, 55.0% and *Gossypium arboreum*, 15.9%) (Fig. 2D).

Among the seven databases, functional annotations with the GO, KOG, and KEGG databases enabled the classification of the unigenes in specific categories, thereby providing a more systemic analysis of the transcriptome output. A total of 59,384 unigenes were classified into GO categories, with "cellular process" from the biological process (BP) category, "binding" from the molecular function (MF) category, and "cell" from the cellular component (CC) category identified as the most enriched GO terms in the three

main categories (Fig. S2). A smaller proportion of unigenes (32,173, 23.51%) were assigned to KEGG pathways (Fig. S3), with ''carbohydrate metabolism'' from the metabolism category and ''translation'' and ''folding, sorting and degradation'' from the genetic information processing category the top three KEGG pathways. Fewer unigenes (20,553 of 136,854 unigenes) were classified based on the KOG categories. Although all 25 KOG categories were represented, ''R: general function prediction only'', ''O: posttranslational modification, protein turnover, chaperons'', and ''J: translation, ribosomal structure and biogenesis'' were the most common (Fig. S4).

For a more specific examination of coding sequences, the transcriptomic data were used as queries for BLAST searches of the Nr and SP databases to predict amino acid sequences. Regarding the unigenes lacking matches with sequences in the Nr or SP databases, their open reading frames were predicted with the ESTScan software (*Iseli, Jongeneel & Bucher, 1999*). The number of unigenes annotated by a BLAST search (58,846 unigenes) was similar to the number of unigenes whose open reading frame was predicted with ESTScan (56,037 unigenes). However, the peptides encoded by the BLAST-annotated unigenes were longer than the ESTScan-predicted peptides (Fig. S5A). Additionally, most of the BLAST-annotated unigenes harbored only the termination codon. In contrast, there was a more even split between the number of ESTScan-predicted sequences with and without the initiation codon and/or the termination codon (Fig. S5B).

Differential expression analyses

To preliminarily reveal the molecular mechanisms underlying kenaf seedling responses to Pb stress, the expressed unigenes were compared between the CK and Pb-stressed samples. A total of 102,475 and 98,637 unigenes were respectively expressed in the CK and Pb-stressed samples, with FPKM values exceeding 0.3. Additionally, 83,003 unigenes were expressed in both samples (Fig. 3A). Overall, 1,697 unigenes were identified as differentially expressed between the CK and Pb-stressed samples (Fig. 3B). A GO enrichment analysis of these 1,697 DEGs indicated the three most enriched GO terms were ''catalytic activity'' and ''oxidoreductase activity'' from the MF category and ''oxidation–reduction process'' from the BP category (Fig. 3C). Moreover, the enriched KEGG pathways among the DEGs that were down-regulated in the Pb-stressed samples were ''glycosphingolipid biosynthesis'', ''photosynthesis'', ''fatty acid elongation'', and ''nitrogen metabolism'' (Fig. 4A). In contrast, ''flavone and flavonol biosynthesis'', ''vitamin B_6 metabolism'', and ''phenylpropanoid biosynthesis'' were the main enriched KEGG pathways among the unigenes with up-regulated expression levels in the Pb-stressed samples (Fig. 4B). The enriched KEGG pathways implied that numerous biological processes that maintain plant growth and development were repressed in kenaf seedlings exposed to Pb stress. The KEGG pathways assigned to the DEGs with up-regulated expression in the Pb-stressed samples may contribute to heavy metal stress responses in kenaf.

To probe the possible master regulators of kenaf seedling responses to Pb stress, the DEGs encoding TFs were investigated. The identified unigenes were predicted to include 2,066 TF-coding genes belonging to 53 TF families (Fig. 5A). Among these TF genes, only 55 from 20 TF families had expression levels that were up- or down-regulated in the Pb-stressed samples

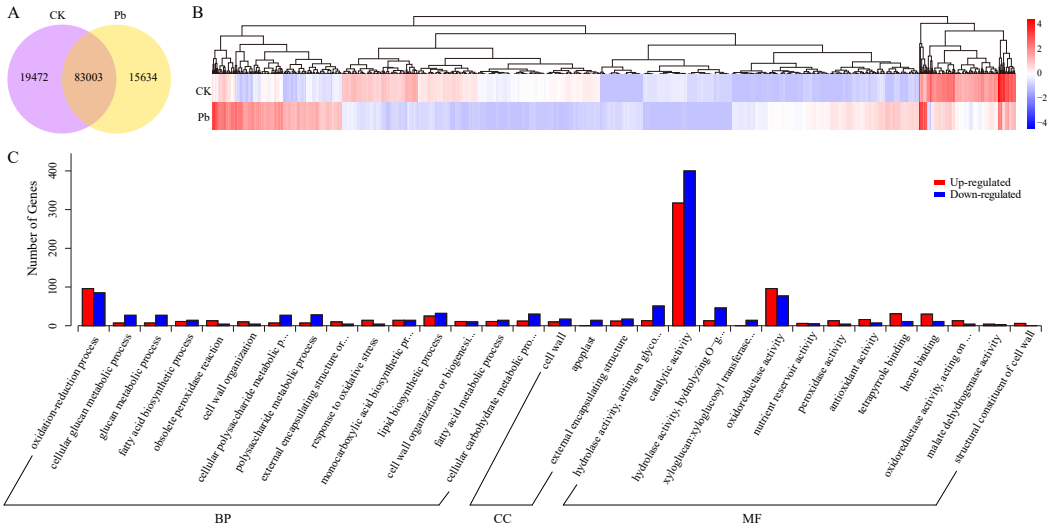

Figure 3 Expression analysis of unigenes. Number of unigenes expressed in CK and Pb stress conditions (A). Diagram of the 1,697 differentially expressed unigenes (DEGs), with blue to red colors representing low to high relative expression levels, respectively (B). Results of the GO enrichment analysis of the up-regulated (red columns) and down-regulated (blue columns) DEGs (C). BP, biological process; CC, cellular component; MF, molecular function.

Full-size DOI: 10.7717/peerj.8733/fig-3

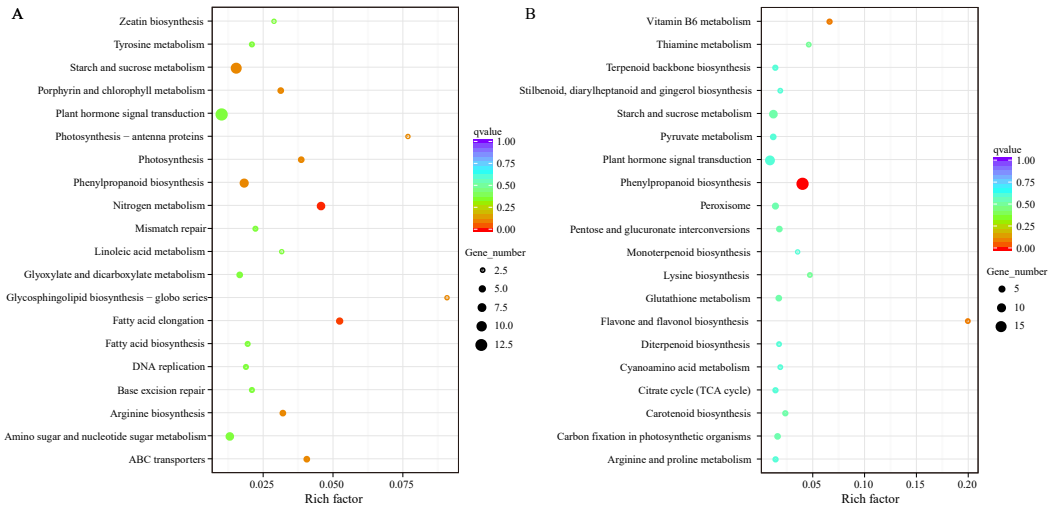

Figure 4 Top 20 enriched KEGG pathways among DEGs. Enriched KEGG pathways among the unigenes with down-regulated expression (A) and up-regulated expression (B) in response to Pb stress.

Full-size DOI: 10.7717/peerj.8733/fig-4

(relative to the corresponding level in the CK samples) (Fig. 5B). A closer examination of these differentially expressed TF (DE-TF) genes revealed that the down- and up-regulated genes were mainly represented by bHLH (basic helix-loop-helix) and NAC family members, respectively. All five NAC DE-TF genes were up-regulated, whereas 11 of the 12 bHLH DE-TF genes were down-regulated. To verify the reliability of the RNA-seq data, eight

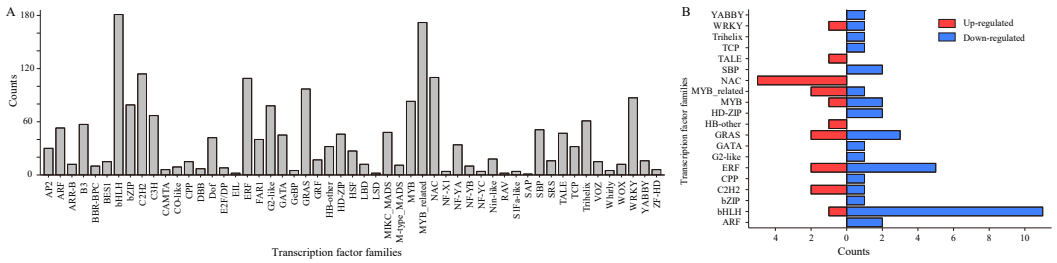

Figure 5 Transcription factors (TFs) examined in the current study. Numbers of predicted TF genes from each TF family among the unigene sequences (A). Differentially expressed TF genes in Pb-stressed compared with CK samples (B).

Full-size DOI: 10.7717/peerj.8733/fig-5

randomly selected DE TF genes in Fig. 5B, including all NAC TF genes (Cluster-5711.10506, Cluster-5711.10507, Cluster-5711.10680, Cluster-5711.108716, and Cluster-5711.35745), two ethylene-responsive element-binding factor (ERF) genes (Cluster-5711.107017 and Cluster-5711.107018), and one teosinte branched1/cincinnata/proliferating cell factor (TCP) gene (Cluster-5711.101858), were analyzed by qRT-PCR. The expression levels of all of these TF genes were higher in the Pb-stressed samples than in the CK samples (Fig. S6), which was consistent with the transcriptome sequencing data.

The NAC TFs in responding the Pb stress

Only 5 of the 110 NAC TF genes predicted based on our transcriptome data (Fig. 5A) were differentially expressed, with Pb stress up-regulating their expression levels (Fig. 5B), implying they have a regulatory role in the kenaf response to Pb stress. The functional annotation of these five kenaf genes (i.e., Cluster-5711.10506, Cluster-5711.10507, Cluster-5711.10680, Cluster-5711.108716, and Cluster-5711.35745) based on the known functions of the corresponding Arabidopsis orthologs (Table S6) suggested the NAC-involved kenaf response to Pb stress is probably dependent on PCD processes. Meanwhile, the MDA content representing the extent of ROS-induced lipid peroxidation (*Ayala, Munoz & Argüelles, 2014*) was significantly higher in the Pb-stressed samples than in the CK samples (Fig. 6A; Table S7). Consistent with this finding, the abundance of PRO, which can increase ROS formation (*Donald et al., 2001*), was also higher under Pb stress conditions than under CK conditions (Fig. 6B; Table S8). Additionally, the activities of the ROS-scavenging enzymes (*Paradiso et al., 2016*), including POD and CAT, decreased following the Pb treatment (Figs. 6C,6D; Tables S9, S10). These results indicated Pb stress increases ROS levels and the expression of PCD-related NAC TF genes in kenaf.

DISCUSSION

Kenaf is a broadly used multi-purpose fiber crop (*Ayadi et al., 2011*). However, there has been minimal fundamental research on this particular species. To date, only a few studies applying RNA-seq approaches have been conducted on kenaf (*Chen et al., 2014*; *Zhang et al., 2015*; *Li et al., 2016*; *Li et al., 2017*), and only one of them focused on transcriptomic responses under adverse conditions (*Li et al., 2017*). Thus, relatively little is

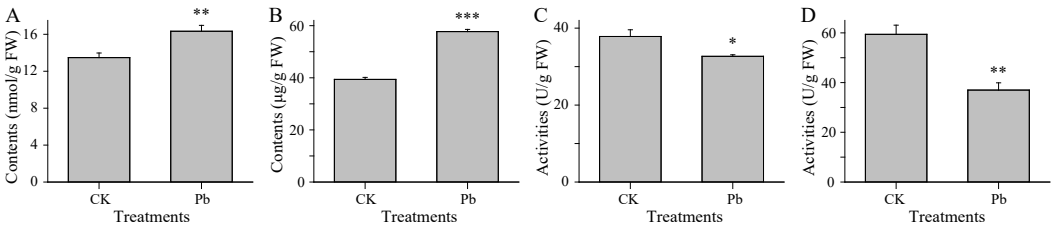

Figure 6 Physiological traits under CK and Pb stress conditions. The MDA (A) and PRO (B) contents as well as the CAT (C) and POD (D) activities are presented on the basis of fresh weight (FW). Error bars represent the standard deviation. Significant differences between the CK and Pb-stressed samples (as determined with Student's *t*-test) are indicated as follows: $^{*}p < 0.05$, $^{**}p < 0.01$, and $^{***}p < 0.001$.
Full-size DOI: 10.7717/peerj.8733/fig-6

known about the effects of diverse environmental conditions on the molecular mechanisms in kenaf. The current study involved a transcriptome analysis of whole kenaf seedlings subjected to normal and plumbic stress conditions, with the resulting data potentially useful for elucidating the stress-induced molecular mechanisms at the transcript level. The 1,697 DEGs between the CK and Pb-stressed samples (Fig. 3B) were grouped at various levels (Figs. 3C, 4). The down-regulated pathways (Fig. 4A), including glycosphingolipid biosynthesis and photosynthesis, are required for plant growth. The glycosphingolipids are pivotal molecules for maintaining cellular communication in multicellular organisms (*D'Angelo et al., 2013*) and photosynthesis is an indispensable source of energy for plants. Thus, plumbic stress appears to suppress critical plant growth processes. In contrast, the up-regulated pathways (Fig. 4B) are likely involved in kenaf responses to adverse conditions. For example, earlier studies proved that diverse flavonoids influence the UV tolerance of rice cultivars and Arabidopsis ecotypes at various latitudes (*Tohge & Fernie, 2016*; *Peng et al., 2017*). Additionally, vitamin B_6 contents have been linked to plant responses to adverse conditions (*Bagri et al., 2018*; *Chandrasekaran & Chun, 2018*; *Nan et al., 2019*). Future studies should focus on the up-regulated pathways as well as the associated unigenes.

Considering the relatively limited molecular research on kenaf, the up-stream regulators of gene expression (i.e., TFs) should be investigated in detail. Accordingly, to identify possible master transcriptional regulators, unigenes encoding TFs were predicted and analyzed (Fig. 5). Many members of various TF families, including MYB (*Li, Ng & Fan, 2015*), bZIP (*Liu & Chu, 2015*), bHLH (*Yadav & Mani, 2019*), TCP (*Ding et al., 2019*), and NAC (*Yuce et al., 2019*) TFs are reportedly involved in plant defenses against abiotic stresses. However, these TFs are also important for plant growth (*Cheng et al., 2019*; *Liu et al., 2019*; *Van Es et al., 2019*), which makes identifying the TFs responsive to Pb stress based solely on our transcriptomic data unlikely. Interestingly, the expression levels of all five detected differentially expressed NAC TF genes were up-regulated following the Pb treatment (Fig. 5B), implying these genes may have regulatory roles affecting kenaf responses to Pb stress. Further analyses suggested these NAC TF genes may be involved in PCD (Table S6), which is a highly regulated and organized cell suicide process crucial for removing damaged or infected cells (*Petrov et al., 2015*). This process is linked to ROS production and accumulation (*Nath & Lu, 2015*). In plants, ROS are always formed from

O_2 because of the inevitable leakage of electrons during the electron transport activities of chloroplasts, mitochondria, and plasma membranes or as a byproduct of various metabolic pathways localized in different cellular compartments (*Rio et al., 2006*; *Blokhina & Fagerstedt, 2010*; *Heyno et al., 2011*). Adverse environmental conditions (e.g., biotic or abiotic stresses) enhance ROS production in plants because of a disruption in cellular homeostasis (*Mittler, 2002*; *Sharma & Dubey, 2005*; *Sharma & Dubey, 2007*; *Maheshwari & Dubey, 2009*; *Srivastava & Dubey, 2011*). In the current study, analyses of MDA and PRO contents and POD and CAT activities (Fig. 6) suggested Pb stress increases ROS levels in kenaf plants. This finding and the observed up-regulated expression of all identified NAC TF genes are possibly associated with PCD (Table S6) and are consistent with the previously established relationship between PCD and ROS (*Nath & Lu, 2015*). Therefore, we speculate that kenaf plants undergo ROS-dependent PCD in response to plumbic stress, with the up-regulated NAC TF genes tuning PCD.

In previous studies, kenaf plants were subjected to Cd (*Li et al., 2013*; *Deng et al., 2017*) and Cr (*Niu et al., 2018*) stresses. However, these investigations focused on plant physiological traits, but not the underlying molecular mechanisms. Consistent with the findings of these earlier studies, we also observed elevated MDA contents (lipid peroxidation) and suppressed POD activities following an exposure to heavy metal stress, which are phenomena that may be associated with ROS-dependent PCD regulated by several NAC TFs. Future detailed examinations of these NAC TFs may help clarify the molecular mechanisms of kenaf plants subjected to various heavy metal stresses. We may also focus on the three KEGG pathways (flavone and flavonol biosynthesis, vitamin B_6 metabolism, and phenylpropanoid biosynthesis) that were significantly enriched in the kenaf seedlings under plumbic stress conditions. The observation that these pathways are affected by Pb stress suggests specific metabolites and/or regulatory genes may influence kenaf tolerance to heavy metals. Indeed, vitamin B_6 metabolites are reportedly responsive to adverse conditions (*Bagri et al., 2018*; *Nan et al., 2019*) and the flavonoid-regulating MYB TFs are known to enhance heavy metal stress resistance (*Ai et al., 2018*; *Raldugina et al., 2018*). Furthermore, the phenylpropanoid pathway is activated to provide protection against heavy metals via the thickening of physical barriers (*Chen et al., 2019*). A comprehensive analysis of the up-regulated NAC TF genes and the unigenes involved in the enriched pathways may provide additional insights into the molecular basis of kenaf responses to excessive amounts of heavy metals.

CONCLUSIONS

Our transcriptome sequencing data generated 44.57 Gb clean reads potentially related to kenaf responses to plumbic stress. To probe the possible master regulators of the underlying molecular mechanism, TF genes were predicted and analyzed. On the basis of our transcriptome data combined with analyses of physiological traits, we propose that kenaf seedlings experience ROS-dependent PCD, which may be regulated by the differentially expressed NAC TF genes. Future studies should characterize the roles of these NAC TFs to provide more detailed insights into the molecular mechanisms mediating kenaf plant responses to plumbic stress.

ADDITIONAL INFORMATION AND DECLARATIONS

Funding

This study was financially supported by the National Natural Science Foundation of China (31801406), the Youth Talent Program of Zhejiang Academy of Agricultural Sciences (2016R25R08E01), the Hangzhou Science and Technology Plan Guidance program (20163501Y79), the China Agriculture Research System (CARS-16-S05), and the Open Project of Key Laboratory of Hemp Biology and Processing of the Ministry of Agriculture (KL-IBFC-201904). The funders had no role in study design, data collection and analysis, decision to publish, or preparation of the manuscript.

Grant Disclosures

The following grant information was disclosed by the authors:
National Natural Science Foundation of China: 31801406.
Youth Talent Program of Zhejiang Academy of Agricultural Sciences: 2016R25R08E01.
Hangzhou Science and Technology Plan Guidance program: 20163501Y79.
China Agriculture Research System: CARS-16-S05.
Open Project of Key Laboratory of Hemp Biology and Processing of the Ministry of Agriculture: KL-IBFC-201904.

Competing Interests

The authors declare there are no competing interests.

Author Contributions

- Xia An conceived and designed the experiments, performed the experiments, analyzed the data, prepared figures and/or tables, authored or reviewed drafts of the paper, and approved the final draft.
- Jie Chen conceived and designed the experiments, analyzed the data, authored or reviewed drafts of the paper, and approved the final draft.
- Guanrong Jin conceived and designed the experiments, authored or reviewed drafts of the paper, and approved the final draft.

Data Availability

The following information was supplied regarding data availability:

All raw data is available at NCBI SRA: SRR9163842. to SRR9163845.

Supplemental Information

Supplemental information for this article can be found online at http://dx.doi.org/10.7717/peerj.8733#supplemental-information.

REFERENCES

Ai TN, Naing AH, Yun BW, Lim SH, Kim CK. 2018. Overexpression of RsMYB1 enhances anthocyanin accumulation and heavy metal stress tolerance in transgenic petunia. *Frontiers in Plant Science* **9**:Article 1388 DOI 10.3389/fpls.2018.01388.

An X, Jin G, Zhang J, Luo X, Chen C, Li W, Ma G, Jin L, Dai L, Shi X, Wei W, Zhu G. 2018. Protein responses in kenaf plants exposed to drought conditions determined using iTRAQ technology. *FEBS Open Bio* **8**:1572–1583 DOI 10.1002/2211-5463.12507.

Anders S, Huber W. 2010. Differential expression analysis for sequence count data. *Genome Biology* **11**:Article R106 DOI 10.1186/gb-2010-11-10-r106.

Ayadi R, Hamrouni L, Hanana M, Bouzid S, Trifi M, Khouja ML. 2011. In vitro propagation and regeneration of an industrial plant kenaf (*Hibiscus cannabinus* L.). *Industrial Crops and Products* **33**:474–480 DOI 10.1016/j.indcrop.2010.10.025.

Ayala A, Muñoz MF, Argüelles S. 2014. Lipid peroxidation: production, metabolism, and signaling mechanisms of malondialdehyde and 4-hydroxy-2-nonenal. *Oxidative Medicine and Cellular Longevity* **2014**:Article 360438.

Bagri DS, Upadhyaya DC, Kumar A, Upadhyaya CP. 2018. Overexpression of PDX-II gene in potato (*Solanum tuberosum* L.) leads to the enhanced accumulation of vitamin B6 in tuber tissues and tolerance to abiotic stresses. *Plant Science* **272**:267–275 DOI 10.1016/j.plantsci.2018.04.024.

Blokhina O, Fagerstedt KV. 2010. Reactive oxygen species and nitric oxide in plant mitochondria: origin and redundant regulatory systems. *Physiologia Plantarum* **138**:447–462 DOI 10.1111/j.1399-3054.2009.01340.x.

Chandrasekaran M, Chun SC. 2018. Vitamin B6 biosynthetic genes expression and antioxidant enzyme properties in tomato against, *Erwinia carotovora* subsp. carotovora. *International Journal of Biological Macromolecules* **116**:31–36 DOI 10.1016/j.ijbiomac.2018.05.024.

Chen H, Li Y, Ma X, Guo L, He Y, Ren Z, Kuang Z, Zhang X, Zhang Z. 2019. Analysis of potential strategies for cadmium stress tolerance revealed by transcriptome analysis of upland cotton. *Scientific Report* **9**:86.

Chen P, Ran S, Li R, Huang Z, Qian J, Yu M, Zhou R. 2014. Transcriptome *de novo* assembly and differentially expressed genes related to cytoplasmic male sterility in kenaf (*Hibiscus cannabinus* L.). *Molecular Breeding* **34**:1879–1891 DOI 10.1007/s11032-014-0146-8.

Cheng L, Han Y, Liu H, Jiang R, Li S. 2019. Transcriptomic analysis reveals ethylene's regulation involved in adventitious roots formation in lotus (*Nelumbo nucifera* Gaertn.). *Acta Physiologiae Plantarum* **41**:e100997.

D'Angelo G, Capasso S, Sticco L, Russo D. 2013. Glycosphingolipids: synthesis and functions. *The FEBS Journal* **280**:6338–6353 DOI 10.1111/febs.12559.

Davidson NM, Oshlack A. 2014. Corset: enabling differential gene expression analysis for *de novo* assembled transcriptomes. *Genome Biology* **15**:Article 410.

Del Río LA, Sandalio LM, Corpas FJ, Palma JM, Barroso JB. 2006. Reactive oxygen species and reactive nitrogen species in peroxisomes. Production, scavenging, and role in cell signaling. *Plant Physiology* **141**:330–335 DOI 10.1104/pp.106.078204.

Deng Y, Li D, Huang Y, Huang S. 2017. Physiological response to cadmium stress in kenaf (*Hibiscus cannabinus* L.) seedlings. *Industrial Crops and Products* **107**:453–457 DOI 10.1016/j.indcrop.2017.06.008.

Ding H, Wang G, Lou L, Lv J. 2016. Physiological responses and tolerance of kenaf (*Hibiscus cannabinus* L.) exposed to chromium. *Ecotoxicology And Environmental Safety* **133**:509–518 DOI 10.1016/j.ecoenv.2016.08.007.

Ding S, Cai Z, Du H, Wang H. 2019. Genome-wide analysis of TCP family genes in *Zea mays* L. identified a role for ZmTCP42 in drought tolerance. *International Journal of Molecular Sciences* **20**:Article 2762 DOI 10.3390/ijms20112762.

Donald SP, Sun XY, Hu CA, Yu J, Mei JM, Valle D, Phang JM. 2001. Proline oxidase, encoded by p53-induced gene-6, catalyzes the generation of proline-dependent reactive oxygen species. *Cancer Research* **61**:1810–1815.

Grabherr MG, Haas BJ, Yassour M, Levin JZ, Thompson DA, Amit I, Adiconis X, Fan L, Raychowdhury R, Zeng Q, Chen Z, Mauceli E, Hacohen N, Gnirke A, Rhind N, Palma FDi, Birren BW, Nusbaum C, Lindblad-Toh K, Friedman N, Regev A. 2011. Trinity: reconstructing a full-length transcriptome without a genome from RNA-Seq data. *Nature Biotechnology* **29**:644–652 DOI 10.1038/nbt.1883.

Heyno E, Mary V, Schopfer P, Krieger-Liszkay A. 2011. Oxygen activation at the plasma membrane: relation between superoxide and hydroxyl radical production by isolated membranes. *Planta* **234**:35–45 DOI 10.1007/s00425-011-1379-y.

Iseli C, Jongeneel CV, Bucher P. 1999. ESTScan: a program for detecting, evaluating, and reconstructing potential coding regions in EST sequences. *Proceedings International Conference on Intelligent Systems for Molecular Biology* **99**:138–148.

Li B, Dewey CN. 2011. RSEM: accurate transcript quantification from RNA-Seq data with or without a reference genome. *BMC Bioinformatics* **12**:323 DOI 10.1186/1471-2105-12-323.

Li C, Ng CK, Fan L. 2015. MYB transcription factors, active players in abiotic stress signaling. *Environmental and Experimental Botany* **114**:80–91 DOI 10.1016/j.envexpbot.2014.06.014.

Li F, Qi J, Zhang G, Lin L, Fang P, Tao A, Xu J. 2013. Effect of cadmium stress on the growth, antioxidative enzymes and lipid peroxidation in two kenaf (*Hibiscus cannabinus* L.) plant seedlings. *Journal of Integrative Agriculture* **12**:610–620 DOI 10.1016/S2095-3119(13)60279-8.

Li H, Li D, Chen A, Tang H, Li J, Huang S. 2016. Characterization of the kenaf (*Hibiscus cannabinus*) global transcriptome using Illumina paired-end sequencing and development of EST-SSR Markers. *PLOS ONE* **11**:e0150548 DOI 10.1371/journal.pone.0150548.

Li H, Li D, Chen A, Tang H, Li J, Huang S. 2017. RNA-seq for comparative transcript profiling of kenaf under salinity stress. *Journal of Plant Research* **130**:365–372 DOI 10.1007/s10265-016-0898-9.

Liu C, Ma H, Zhou J, Li Z, Peng Z, Guo F, Zhang J. 2019. TsHD1 and TsNAC1 cooperatively play roles in plant growth and abiotic stress resistance of. *The Plant Journal* **99**:81–97 DOI 10.1111/tpj.14310.

Liu X, Chu Z. 2015. Genome-wide evolutionary characterization and analysis of bZIP transcription factors and their expression profiles in response to multiple abiotic stresses in *Brachypodium distachyon*. *BMC Genomics* **16**:227 DOI 10.1186/s12864-015-1457-9.

Livak KJ, Schmittgen TD. 2001. Analysis of relative gene expression data using real-time quantitative PCR and the 2(-Delta Delta C(T)) Method. *Methods* **25**:402–408 DOI 10.1006/meth.2001.1262.

Maheshwari R, Dubey RS. 2009. Nickel-induced oxidative stress and the role of antioxidant defence in rice seedlings. *Plant Growth Regulation* **59**:37–49 DOI 10.1007/s10725-009-9386-8.

Mao X, Cai T, Olyarchuk JG, Wei L. 2005. Automated genome annotation and pathway identification using the KEGG Orthology (KO) as a controlled vocabulary. *Bioinformatics* **21**:3787–3793 DOI 10.1093/bioinformatics/bti430.

Mittler R. 2002. Oxidative stress, antioxidants and stress tolerance. *Trends in Plant Science* **7**:405–410 DOI 10.1016/S1360-1385(02)02312-9.

Nan N, Wang J, Shi Y, Qian Y, Jiang L, Huang S, Liu Y, Wu Y, Liu B, Xu Z. 2019. Rice plastidial NAD-dependent malate dehydrogenase 1 negatively regulates salt stress response by reducing the vitamin B6 content. *Plant Biotechnology Journal* **18(1)**:172–184 DOI 10.1111/pbi.13184.

Nath K, Lu Y. 2015. A paradigm of reactive oxygen species and programed cell death in plants. *Journal of Cell Science and Therapy* **6**:Article 2.

Niu L, Cao R, Kang J, Zhang X, Lv J. 2018. Ascorbate-glutathione cycle and ultrastructural analyses of two kenaf cultivars (*Hibiscus cannabinus* L.) under chromium stress. *International Journal of Environmental Research and Public Health* **15**:E1467 DOI 10.3390/ijerph15071467.

Niu X, Xu J, Chen T, Tao A, Qi J. 2016. Proteomic changes in kenaf (*Hibiscus cannabinus* L.) leaves under salt stress. *Industrial Crops and Products* **91**:255–263 DOI 10.1016/j.indcrop.2016.07.034.

Paradiso A, Caretto S, Leone A, Bove A, Nisi R, Gara L de. 2016. ROS Production and scavenging under anoxia and re-oxygenation in Arabidopsis cells: a balance between redox signaling and impairment. *Frontiers in Plant Science* **7**:Article 1803.

Peng M, Shahzad R, Gul A, Subthain H, Shen SQ, Lei L, Zheng ZG, Zhou JJ, Lu DD, Wang SC, Nishawy E, Liu XQ, Tohge T, Fernie AR, Luo J. 2017. Differentially evolved glucosyltransferases determine natural variation of rice flavone accumulation and UV-tolerance. *Nature Communications* **8**:Article 1975 DOI 10.1038/s41467-017-02168-x.

Petrov V, Hille J, Mueller-Roeber B, Gechev TS. 2015. ROS-mediated abiotic stress-induced programmed cell death in plants. *Frontiers in Plant Science* **6**:Article 69.

Raldugina GN, Maree M, Mattana M, Shumkova G, Mapelli S, Kholodova VP, Karpichev IV, Kuznetsov VV. 2018. Expression of rice OsMyb4 transcription factor improves tolerance to copper or zinc in canola plants. *Biologia Plantarum* **62**:511–520 DOI 10.1007/s10535-018-0800-9.

Sharma P, Dubey RS. 2005. Drought induces oxidative stress and enhances the activities of antioxidant enzymes in growing rice seedlings. *Plant Growth Regulation* **46**:209–221 DOI 10.1007/s10725-005-0002-2.

Sharma P, Dubey RS. 2007. Involvement of oxidative stress and role of antioxidative defense system in growing rice seedlings exposed to toxic concentrations of aluminum. *Plant Cell Reports* **26**:2027–2038 DOI 10.1007/s00299-007-0416-6.

Srivastava S, Dubey RS. 2011. Manganese-excess induces oxidative stress, lowers the pool of antioxidants and elevates activities of key antioxidative enzymes in rice seedlings. *Plant Growth Regulation* **64**:1–16 DOI 10.1007/s10725-010-9526-1.

Tohge T, Fernie AR. 2016. Specialized metabolites of the flavonol class mediate root phototropism and growth. *Molecular Plant* **9**:1554–1555 DOI 10.1016/j.molp.2016.10.019.

Trapnell C, Williams BA, Pertea G, Mortazavi A, Kwan G, Van Baren MJ, Salzberg SL, Wold BJ, Pachter L. 2010. Transcript assembly and quantification by RNA-Seq reveals unannotated transcripts and isoform switching during cell differentiation. *Nature Biotechnology* **28**:511–515 DOI 10.1038/nbt.1621.

Van Es SW, Van der Auweraert EB, Silveira SR, Angenent GC, Van Dijk ADJ, Immink RGH. 2019. Comprehensive phenotyping reveals interactions and functions of Arabidopsis thaliana TCP genes in yield determination. *The Plant Journal* **99**:316–328.

Xu Z, Dong M, Peng X, Ku W, Zhao Y, Yang G. 2019. New insight into the molecular basis of cadmium stress responses of wild paper mulberry plant by transcriptome analysis. *Ecotoxicology And Environmental Safety* **171**:301–312 DOI 10.1016/j.ecoenv.2018.12.084.

Yadav BS, Mani A. 2019. Analysis of bHLH coding genes of *Cicer arietinum* during heavy metal stress using biological network. *Physiology And Molecular Biology of Plants* **25**:113–121 DOI 10.1007/s12298-018-0625-1.

Young MD, Wakefield MJ, Smyth GK, Oshlack A. 2010. Gene ontology analysis for RNA-seq: accounting for selection bias. *Genome Biology* **11**:Article R14 DOI 10.1186/gb-2010-11-2-r14.

Yuce M, Taspinar MS, Aydin M, Agar G. 2019. Response of NAC transcription factor genes against chromium stress in sunflower (*Helianthus annuus* L.). *Plant Cell, Tissue and Organ Culture* **136**:479–487 DOI 10.1007/s11240-018-01529-8.

Zhang L, Wan X, Xu J, Lin L, Qi J. 2015. *De novo* assembly of kenaf (*Hibiscus cannabinus*) transcriptome using Illumina sequencing for gene discovery and marker identification. *Molecular Breeding* **35**:Article 192.